The energy-deposition model: electron loss of heavy ions in collisions with neutral atoms at low and intermediate energies

V.P. Shevelko[1*], D. Kato[2], M.S. Litsarev[1] and H. Tawara[2,3]

[1] P.N. Lebedev Physical Institute, Leninskii prospect 53, 119991 Moscow, Russia
[2] National Institute for Fusion Science, Toki 509-5292, Japan
[3] National Institute for Radiological Science, Inage 263-8555, Japan

PACS: 34.50Fa; 34.50.Bw; 29.27.Eg

Abstract

Single- and multiple-electron loss processes in collisions of heavy many-electron ions (positive and negative) in collisions with neutral atoms at low and intermediate energies are considered using the energy-deposition model. The DEPOSIT computer code, created earlier to calculate electron-loss cross sections at high projectile energies, is extended for low and intermediate energies. A description of a new version of DEPOSIT code is given, and the limits of validity for collision velocity in the model are discussed.. Calculated electron-loss cross sections for heavy ions and atoms (N^+, Ar^+, Xe^+, U^+, U^{28+}, W, W^+, Ge^-, Au^-), colliding with neutral atoms (He, Ne, Ar, W) are compared with available experimental and theoretical data at energies E > 10 keV/u. It is found that in most cases the agreement between experimental data and the present model is within a factor of 2. Combining results obtained by the DEPOSIT code at low and intermediate energies with those by the LOSS-R code at high energies (relativistic Born approximation), recommended electron-loss cross sections in a wide range of collision energy are presented.

Key words: loss cross sections, heavy ions, energy-deposition model, rate coefficients

---

* Corresponding author. Tel.: +7-499-7833684; fax: +7-499-1352408. *E-mail address*: v.chevelko@gsi.de (V.P. Shevelko).

1. Introduction

In ion-atom collisions, the interactions between colliding particles depend mainly on their atomic structure and the ion energy. At low energies, the electron capture (EC) is the most dominant process, particularly, for highly charged projectile ions, meanwhile the electron loss (EL) of projectile, often called projectile ionization or stripping,

$$X^{q+} + A \rightarrow X^{(q+m)+} + \Sigma A + me^- \qquad (1)$$

prevails at higher energy range (see, e.g., [1]). Here X^{q+} denotes the projectile ion and m the number of ejected electrons. ΣA means that the target atom can be excited or even ionized.

At low energies, E < 50 keV/u, experimental data on EL processes involving many-electron systems are very limited (see, e.g., [2, 3], meanwhile theoretical analysis of such processes is very complicated and results are even scarcer than experimental data (see, e.g., [4 – 7]). A few theoretical models to calculate the EL cross sections at low collision energies have been reported [4, 6], however, in many cases their results show significant overestimation of experimental data. For relatively high energies E > 1 MeV/u, extensive calculations of single-

and multiple-electron loss cross sections of heavy ions by atomic and molecular targets have been performed using the Classical-trajectory Monte Carlo (CTMC) method (see, e.g., [8 - 10]).

The classical *energy-deposition model*, originally suggested by N. Bohr [11], was successfully applied for ionization of *atoms* by ions in relatively high collision energies and, combining with statistical theory for multi-electron ionization probabilities [12], leads to quite reasonable results for the total and partial (*m*-fold) ionization cross sections of the target atoms (see [13, 14]).

At very low collision energies, a quasi-molecule model based on the adiabatic approximation for one electron in the two-Coulomb-centre system, is used for calculating EL cross sections (ARSENY code [15]), but this model is applied mainly for light projectiles and light targets.

Quite recently [16], the scaling formulae, based on available experimental data, were presented for single- and multiple-electron loss form arbitrary projectile in collisions with neutral atoms over a broad energy range from a few keV/u to hundreds of MeV/u.

Importance of slow ion-atom collisions has recently been realized in a number of applications, particularly, in material sciences based upon low-temperature plasma technologies [17, 18]. For example, in the edge plasma region of the fusion plasma machines like tokamaks, whose temperatures are much lower compared with the a hot plasma at central region, there are a number of low-charged heavy impurity ions, like Ni, Fe and Cr, which are originally sputtered away from the device walls and ionized. Then, they flow into the main plasma region, where they become highly ionized, resulting in enhanced radiation losses and, finally, cooling the high temperature plasmas.

In our previous paper [19], the energy-deposition model based on the semi-classical approximation, was applied for EL of projectiles in collisions with neutral atoms at relatively high energies (E > 1 MeV/u) and a DEPOSIT code was created for systematic calculations of the EL cross sections including multiple-electron losses. It was found that the code can reproduce reasonably well the experimental data in fast ion-atom collisions within a factor of 2, indicating that the code is generally reliable in describing most of the observations, analyzing related phenomena and in its applications.

In the present work we extend the application of the existing version of the DEPOSIT code to low and intermediate energy ranges so that it can now be used from low energies of about 1 keV/u up to the high-energy Born range. At low energies, similarly to high energies, the energy deposited to the projectile by collision with a neutral atom is expressed via 3D-integral over the projectile-ion space. For intermediate energy, a semi-empirical method of calculating the deposited energy is suggested. New formulae are realized in the new version of the DEPOSIT code described in this paper. The results of the relativistic Born calculations, performed by the LOSS-R code [20], are also given to get the upper limit of the total EL cross sections. Finally, multiple-electron loss cross sections are calculated at low energies and compared with available experimental data.

The atomic units $m_e = e = \hbar = 1$ are used where m_e and e denote the electron mass and charge, respectively, and $\hbar$ the Planck constant.

2. Application of the energy-deposition model at low energies

2.1 Basic formulae

In the work [19], single- and multi-electron loss processes were considered in the energy-deposition model for energetic ions colliding with neutral atoms provided that the relative

velocity v is much higher than the ion orbital velocities, i.e. $v >> v_{orb}$. In the present paper, an opposite case is considered, namely, when the velocity v is much smaller than the orbital velocities, $v << v_{orb}$,. In principle, the low-energy electron-loss processes should be treated within a molecular approach such as adiabatic approximation (see, e.g., [15]). However, for collisions of heavy, like Xe^+ + Ar, W^+ + W, U^{4+} + Xe, the molecular treatment for such multi-electron systems can be hardly realized. Therefore, for low-energy heavy particle collisions we again apply the energy-deposition model as we did for high-energy collisions in [19] but using another physical assumptions.

Let us first consider the kinetic energy ΔE_γ which one bound (active) electron from the shell γ of the projectile can gain in a single collision with a neutral target atom:

$$\Delta E_\gamma = \frac{(u_\gamma + \Delta u_\gamma)^2}{2} - \frac{u_\gamma^2}{2} = u_\gamma \Delta u_\gamma + \frac{(\Delta u_\gamma)^2}{2} , \qquad (2)$$

where u_γ and Δu_γ denote the orbital velocity and its gain due to collision with a neutral atom, respectively.
The values u_γ and Δu_γ are obtained from the classical equations:

$$u_\gamma = \sqrt{2I_\gamma} , \qquad (3)$$

$$\Delta u_\gamma = \int_{-\infty}^{\infty} \frac{dU(R)}{dp} dt = \int_{-\infty}^{\infty} \frac{dU(R)}{dR} \frac{dR}{dp} dt . \qquad (4)$$

Here I_γ denotes the binding energy of the projectile shell γ, $U(R)$ the field of a neutral atom at a distance R from its nucleus, t the time and p the impact parameter between the active electron and the target nucleus.

In the case of high velocities, $v >> u_\gamma$, the velocity gain $\Delta u_\gamma \sim 2v$ [21], u_γ is small and one can neglect the linear term on Δu_γ in eq. (2). Then the deposited energy $\Delta E_\gamma(p)$ is defined by the quadratic term of eq. (2):

$$\Delta E_\gamma(p) = \frac{(\Delta u_\gamma)^2}{2}, \quad v >> u_\gamma . \qquad (5)$$

In the opposite case of low velocities, $v << u_\gamma$, the first linear term prevails because $\Delta u_\gamma \sim v$, u_γ is large and the deposited energy $\Delta E_\gamma(p)$ is given by a linear term of the velocity gain Δu_γ:

$$\Delta E_\gamma(p) = u_\gamma \Delta u_\gamma, \quad v << u_\gamma . \qquad (6)$$

The field $U(R)$ of the target neutral atom can be presented in a close analytical form as a sum of three Yukawa potentials with six fitting parameters obtained from the Dirac-Hartree-Fock-Slater calculations [22]:

$$U(R) = -\frac{Z}{R} \sum_{i=1}^{3} A_i e^{-\alpha_i R}, \quad \sum_{i=1}^{3} A_i = 1 , \qquad (7)$$

where A_i and α_i denote the fitting parameters and Z the nuclear charge of the neutral target atom (also a number of the target electrons).

Using a straight-line trajectory approximation

$$R^2 = p^2 + \mathrm{v}_\mathrm{r}^2 t^2 \tag{8}$$

and representation (7) for the atomic field, the energy deposited to one active projectile electron at low velocities v can be written in the form:

$$\Delta E_\gamma(p) = \frac{2u_\gamma Z}{\mathrm{v}_\mathrm{r} p}\sum_{i=1}^{3} A_i F_A(\alpha_i p),\ \mathrm{v}_\mathrm{r} = \sqrt{\mathrm{v}^2 + u_\gamma^2}, \tag{9}$$

$$F_A(k) = \int_0^\infty dy\ k^2 e^{-\sqrt{k^2+y^2}}\left[\frac{1}{(k^2+y^2)^{3/2}} + \frac{1}{(k^2+y^2)}\right]\ , \tag{10}$$

where v_r denotes the relative velocity, and the function F_A(k) is normalized to unity at $k \to 0$ (see [19]):

$$F_A(k) \approx 1 - 0.285k + ...,\ \ k \to 0\,. \tag{11}$$

According to eq. (9), the deposited energy $\Delta\mathrm{E}_\gamma(p)$ diverges at $p \to 0$ and, therefore, $\Delta\mathrm{E}_\gamma$(p) should be normalized at p = 0. In the paper [19], where the fast collisions, v >> u_γ, are considered, the deposited energy $\Delta\mathrm{E}_\gamma(p)$ was normalized to the maximum energy $\Delta\mathrm{E}_\gamma^{\max}$ which an active electron can gain in a head-on collision with the atomic nucleus:

$$\Delta E_{high}^{\max} = \Delta E_\gamma(p=0) = 2\mathrm{v}^2\,. \tag{12}$$

To find the $\Delta\mathrm{E}_\gamma^{\max}$ value for slow collisions, we use assumptions similar to those made in the paper [5], i.e., the energy transferred to the active electron is mainly due to collisions with the target electrons but not with its atomic nucleus because the projectile electrons can adjust adiabatically to the slow nuclear motion of colliding particles. The maximum energy $\Delta\mathrm{E}_\gamma^{\max}$ can be found from a simple consideration that each projectile shell has its own mean radius r_γ, then it is easy to obtain:

$$\Delta E_{slow}^{\max} = \Delta E_\gamma(p=0) = N_{eff}^{(\gamma)}\frac{\mathrm{v}^2}{2}, \tag{13}$$

$$N_{eff}^{(\gamma)} \approx \begin{cases} Z\dfrac{r_\gamma^2}{R_A^2},\ r_\gamma \le R_A \\ Z,\ r_\gamma > R_A \end{cases}\ , \tag{14}$$

where R_A denotes a radius of the target atom. The factor $\mathrm{v}^2/2$ corresponds to the energy deposited to the projectile active electron by a single collision with one target electron so that the $N^{(\gamma)}_{\mathrm{eff}}$ is a number of effective head-on collisions (p = 0) of a projectile electron from the shell γ with a target electron gas within a cylinder of diameter $2r_\gamma$.

According to eq. (14) the number of effective collisions does not exceed the total number of the target electrons. The assumption (13) is quite rough but allows one to get reasonable results as will be shown below. The alternative way to find $N^{(\gamma)}_{\mathrm{eff}}$ is to use a model suggested in [5] using two overlapping spheres of colliding particles but this model requires five additional assumptions and two fitting parameters which can be obtained only from experimental data. We choose the semi-classical energy-deposition model which is free from any fitting parameters.

In the classical energy-deposition model the total energy $T(b)$ transferred to all projectile electrons by the target atom is given by

$$T(b)=\sum_{\gamma}\int \rho(r)\,\Delta E_{\gamma}(p)\,d^{3}r, \tag{15}$$

where $\rho(r)$ denotes the electron density of the projectile ion at the distance r from its nucleus and b the impact parameter between nuclei of two colliding particles. The sum over γ means summation over all shells of the projectile. With account for normalization given by eqs. (13, 14), the energy $\Delta E_{\gamma}(p)$ transferred to one projectile electron at low energies can be presented in the form:

$$\Delta E_{\gamma}(p)=\frac{2N_{eff}^{(\gamma)}u_{\gamma}\sum_{i=1}^{3}A_{i}F_{A}(\alpha_{i}p)}{\mathrm{v}_{\mathrm{r}}\left[p+\dfrac{4u_{\gamma}}{\mathrm{v}_{\mathrm{r}}\mathrm{v}^{2}}\right]},\quad \mathrm{v}_{\mathrm{r}}=\sqrt{\mathrm{v}^{2}+u_{\gamma}^{2}}\qquad . \tag{16}$$

The $F_{\mathrm{A}}(\mathrm{k})$ function is given by eq. (10). In the case of a straight-line trajectory approximation (8), b, p and r values are related by a simple geometrical equation given in [19]. In the present model, the target atomic potential $U(\mathrm{R})$ is considered to be unchanged during the collision time.

The electron density $\rho(r)$ in eq. (15) is normalized to the total number of the projectile electrons N:

$$\int_{0}^{\infty}\rho(r)\,dr=N\,. \tag{17}$$

According to the energy-deposition model, electron loss of the projectile can occur only if the total energy $T(\mathrm{b})$, deposited to the whole projectile ion, is larger than its first ionization potential I_1, i.e.

$$T(b)\geq I_{1}\,. \tag{18}$$

The total electron-loss cross section of the projectile by neutral atom, i.e., summed over many-fold (m) electron-loss cross sections, is given by

$$\sigma_{tot}(\mathrm{v})=\sum_{m=1}^{N}\sigma_{m}=\pi b_{\max}^{2}\quad , \tag{19}$$

where $b_{\max}$ is the maximum impact parameter, at which the active electron can be ionized, and is found from equation:

$$T(b_{\max})=I_{1}\quad . \tag{20}$$

2.2 Validity conditions for the energy-deposition model at low energies

At low velocities v, the first linear term in eq. (2) prevails so that one has

$$u_{\gamma}\Delta u_{\gamma}>>\frac{(\Delta u_{\gamma})^{2}}{2}\ , \tag{21}$$

from which we can estimate the upper limit of validity for velocity v. Actually, from eqs. (13), (14) and (21) one gets:

$$\mathrm{v}^2 << \frac{2u_\gamma}{\sqrt{Z}} \frac{R_A}{r_\gamma} . \tag{22}$$

Assuming that at low energies the main contribution comes from the loss of the outermost projectile electrons with the ionization potential I_1, one has from eq. (22):

$$\mathrm{v} << \frac{2R_A}{R_{ion}} \left(\frac{2I_1}{Z} \right)^{1/2} , \tag{23}$$

where R_{ion} denotes the mean radius of the projectile. Typical mean radii for some ions and atoms of interest are given in Table 1.

Table 1. The mean radii of positive ions, R_{ion}, calculated by the ATOM code [23], and neutral atoms, R_A, taken from relativistic Dirac-Fock calculations [24] (all in a_0 units). I_1 denotes the first ionization potential (in eV).

Ion	I_1 [eV]	R_{ion} [a_0]	Atom	I_1 [eV]	R_A [a_0]
Ar^{6+}	124	0.99	H	13.6	1.50
Ar^{8+}	422	0.36	He	24.6	0.93
Xe^{18+}	573	0.60	N	14.5	1.44
Pb^{25+}	814	0.52	Ne	21.6	0.97
U^{5+}	62.5	2.33	Ar	15.8	1.65
U^{10+}	158	1.80	Kr	14.0	1.92
U^{28+}	918	0.73	Xe	12.1	2.24
W^{+}	15.0	3.22	W	7.86	3.40
Ge^{-}	1.23	-	C	11.3	1.74
Au^{-}	2.31	-	O	13.6	1.24

It is also possible to estimate a lower limit for validity of approximation at low collision energies. From eqs. (15), (13) and (18) one has:

$$\mathrm{v} \geq \frac{R_A}{\left(\sum_\gamma N_\gamma r_\gamma^2 \right)^{1/2}} \left(\frac{2I_1}{Z} \right)^{1/2} , \tag{24}$$

where the summation is made over *all* subshells γ of the projectile with the number N_γ of equivalent electrons in the shell.

3. New version of the DEPOSIT code

Using the energy-deposition model, it is possible to obtain analytical formulae for the energy T(b) transferred to the projectile at both high [19] and low (section 2.1) relative velocities when

the problem is reduced to numerical calculation of the 3D-integral over the projectile-ion space. Unfortunately, it was not possible to obtain the normalization energy $\Delta E_\gamma^{\max}$ at $p \to 0$ for intermediate velocities when $v \sim v_\gamma$. However, below we suggest a semi-empirical method for calculations of EL cross sections at intermediate velocities.

Let us define the energy $\Delta E_\gamma(p)$ in it by two equations depending on the ratio between v and u_γ:

$$\Delta E_\gamma(p) = \begin{cases} \dfrac{2N_{eff}^{(\gamma)} u_\gamma \sum_{i=1}^{3} A_i F_A(\alpha_i p)}{v_r\left[p + \dfrac{4u_\gamma}{v_r v^2}\right]}, & v \le u_\gamma, \\ \dfrac{2Z^2\left[\sum_{i=1}^{3} A_i F_A(\alpha_i p)\right]^2}{v^2(p^2 + Z^2/v^4)}, & v > u_\gamma \end{cases} . \qquad (25)$$

The lower equation in (25) was used in [19] to describe electron loss at high velocities.

For simplicity, let us consider an electron loss of Ar^+ ions colliding with some atom. This ion has K, L and M electron shells ($1s^2$, $2(sp)^8$ and $3(sp)^7$) with the corresponding set of average orbital velocities u_γ: $u_K = 15.4$, $u_L = 4.5$ and $u_M = 1.2$ a.u. According to eq. (16), the total deposited energy $T_{Ar+}(b)$ is given by the sum over all three shells:

$$T_{Ar^+}(b) = T_K(b) + T_L(b) + T_M(b) \ . \qquad (26)$$

If the relative velocity is small, e.g., v = 0.5 a.u., a contribution from all shells is calculated by the upper formula in eq. (25). If velocity is large, e.g., v = 16 a.u., then the lower formula of eq. (25) is used. If v = 6 a.u., a contribution from the K shell is calculated using the upper formula and from K and M shells by the lower formula of (25), respectively. Such procedure of dividing shells into two groups depending on ratio between velocities v and u_γ allows one to provide effectively a smooth transition of T(b) from low to high velocities and, therefore, to calculate the deposited energy T(b) at all energies.

We note that such dividing electron shells into two groups with different velocities is used in atomic physics, for example, in the works [25]. There, in considering interactions of fast ions with solids, the target electrons are divided into two groups: one of the outmost electrons, described as an electron gas in the valence band, and another one of the inner-shell electrons described by the bound-state wave functions.

Equations (15) and (25) are realized in a new version of the DEPOSIT code which now is intended to calculate the deposited energies T(b), the total- (σ_{tot}) and m-fold (σ_m) electron loss cross sections of positive, negative ions and neutral atoms colliding with *neutral* atoms at low, intermediate and high relative velocities. We remind that the previous version of the DEPOSIT code [19] was used only for calculations at high velocities $v >> v_\gamma$.

4. Numerical calculations and comparison with experiment

In the present work, the total EL cross sections are calculated using eqs. (15) and (25) and *m*-fold cross sections using for the usual formula in the independent-particle model:

$$\sigma_m(\mathrm{v}) = 2\pi \int_0^\infty P_m(b)\, b\, db \qquad . \tag{27}$$

Here $P_m(b)$ denote the *m*-fold electron-loss (ionization) probabilities which were calculated in the Russek statistical model [12]. To calculate the projectile electron density $\rho(r)$ in eq. (15), the Slater radial nodeless wave functions are used (see [19]).

The results of calculations by the DEPOSIT code are compared with available experimental data and CTMC calculations in a wide range of collision energies. We note that in the work [2], the experimental data are compiled only for the partial (not total) EL cross sections σ_m, therefore, the total experimental data mentioned in the figure captions from [2] correspond to the sum of σ_m values.

At high-energy range, the results for EL cross sections in the relativistic Born approximation (the LOSS-R code) are also given to show a high-energy limit of the total EL cross sections. The recommended EL cross sections σ_{rec} over a wide range of the collision energy are also displayed in the figures which were obtained using the following formula:

$$\frac{1}{\sigma_{rec}} = \frac{1}{\sigma_{low}} + \frac{1}{\sigma_{high}}. \tag{28}$$

Here σ_{low} and σ_{high} denote the cross sections calculated by the DEPOSIT and the LOSS-R codes, respectively. The LOSS-R code is originally intended for calculation of the single-EL cross section in the Born approximation and is quite reliable at high collision energies (see [20] for details) including relativistic energy range. Besides, it is well known experimentally and theoretically that at high energies single-electron loss gives the main contribution to the total EL cross sections (see, e.g., [8, 9]).

4.1 The total EL cross sections

Experimental and calculated total EL cross sections of singly charged positive ions colliding with atomic gases are shown in Figs. 1 – 5 at collision energy range from about 10 keV/u to 10 MeV/u. There is quite good agreement with experimental data within a factor of 2 or better. Typically, the data by the DEPOSIT code are larger than experimental data except for the case of Ar^+ + Ne collisions at energies below maximum (Fig. 2). CTMC cross sections decrease more slowly and are larger than the Born EL cross sections (Figs. 2 and 3).

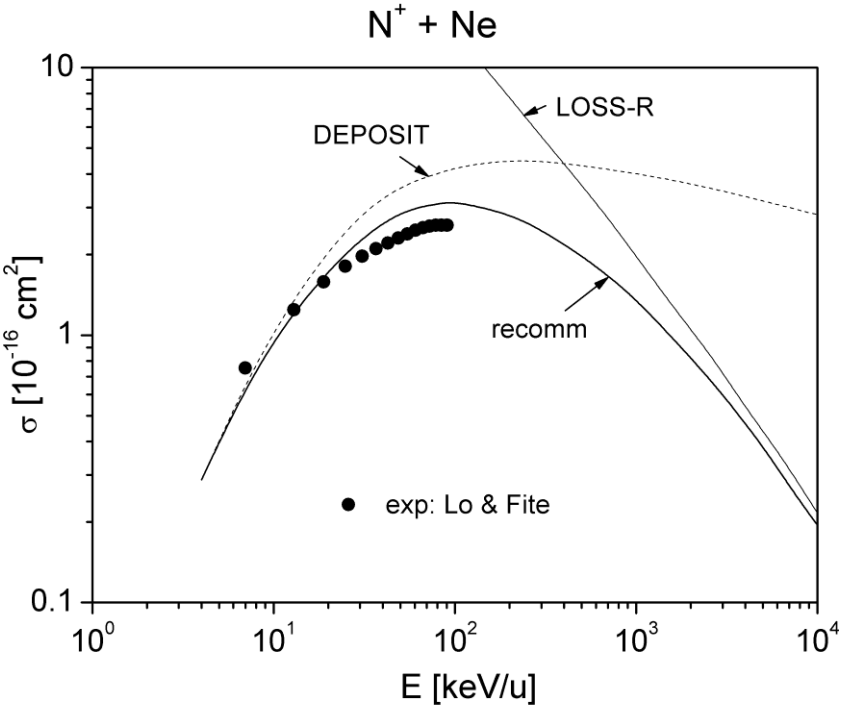

Fig. 1. Total electron-loss cross sections of N^+ ions by Ne atoms as a function of the ion energy. Experiment: solid circles – estimated from [2]. Theory: dashed curve – DEPOSIT code, thin solid curve – LOSS-R code, thick solid curve – recommended cross section, eq. (28).

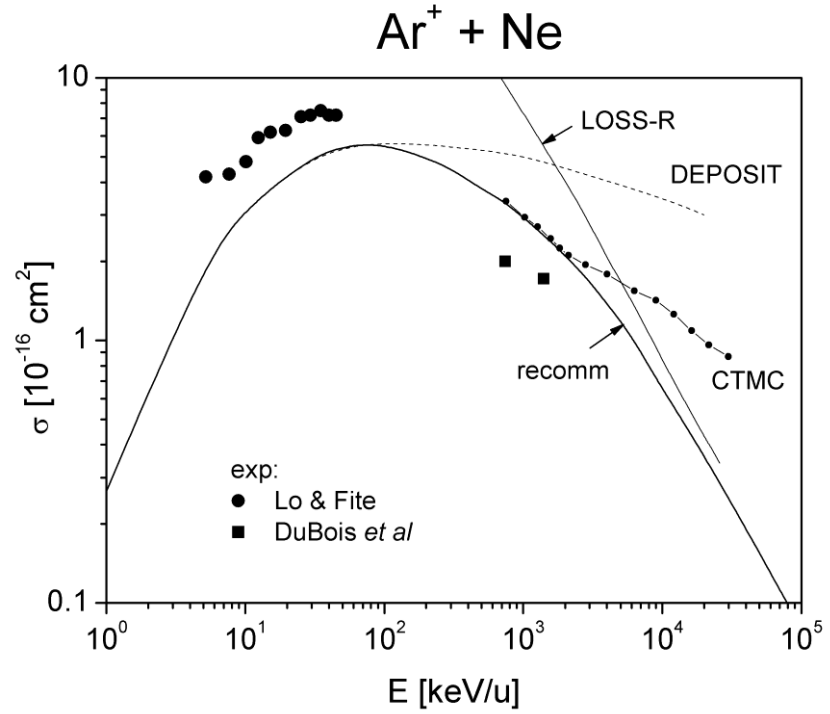

Fig. 2. Total electron-loss cross sections of Ar^+ ions by Ne atoms as a function of the ion energy. Experiment: circles – estimated from [2], squares [10]. Theory: solid curve with circles – CTMC [10], dashed curve – DEPOSIT code, thin solid curve – LOSS-R code, thick solid curve – recommended cross section, eq. (28).

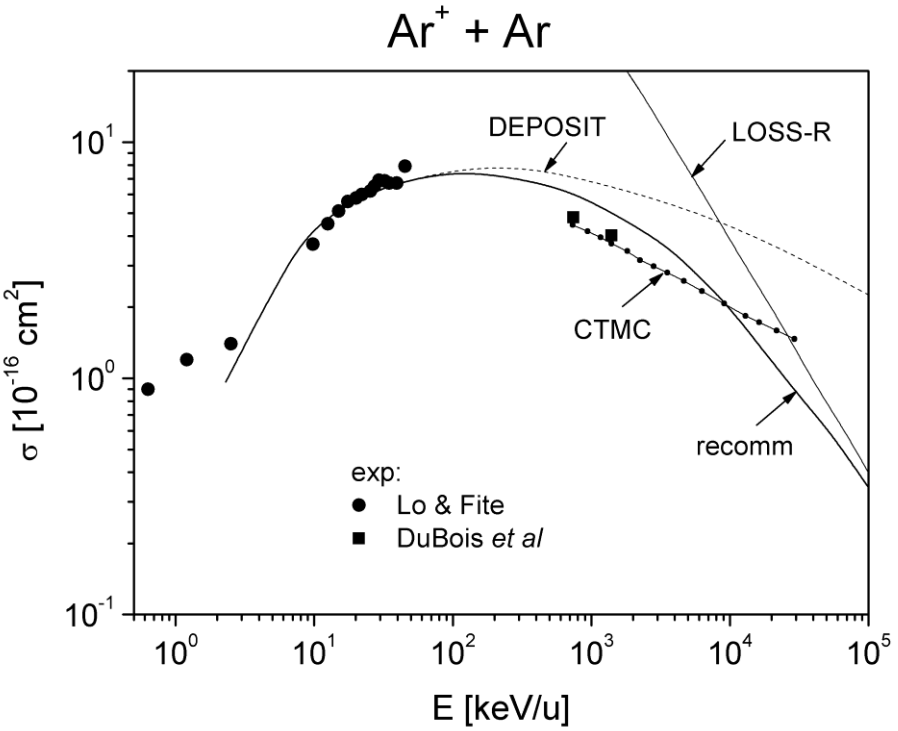

Fig. 3. Total electron-loss cross sections of Ar^+ ions by Ar atoms as a function of the ion energy. Experiment: solid circles – estimated from [2], solid squares [10]. Theory: solid curve with small circles – CTMC [10], dashed curve – DEPOSIT code, thin solid curve – LOSS-R code, thick solid curve – recommended cross section, eq. (28).

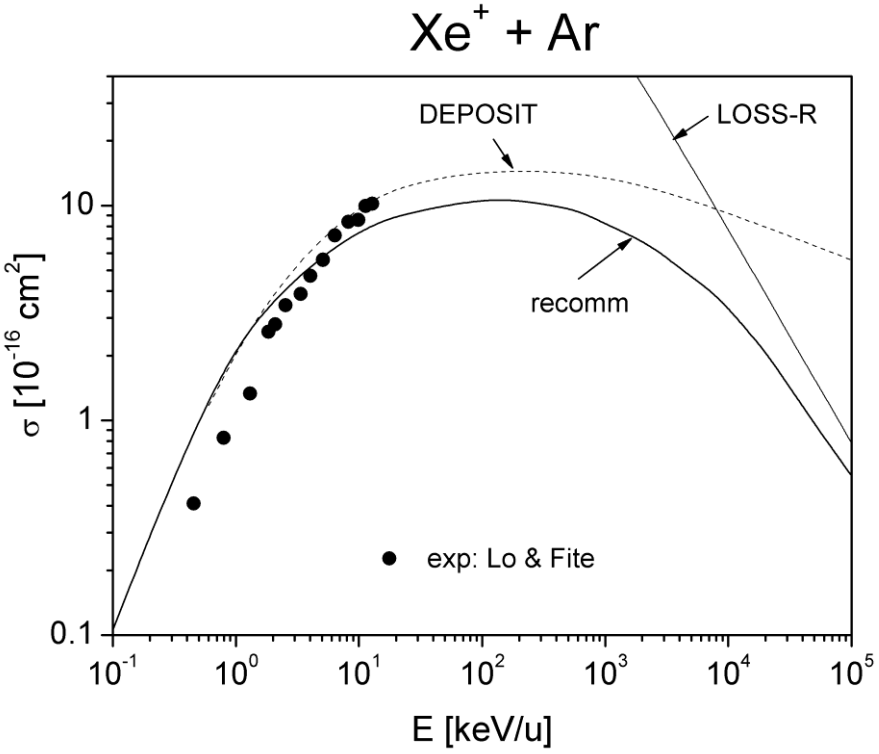

Fig. 4. Total electron-loss cross sections of Xe^+ ions by Ar atoms as a function of the ion energy. Experiment: solid circles – estimated from [3]. Theory: dashed curve – DEPOSIT code, thin solid curve – LOSS-R code, thick solid curve – recommended cross section, eq. (28).

Collisions of U^+ ions with Ar are of a special interest for accelerator physics in view of the International FAIR project [26]. For this case, the results of the DEPOSIT and LOSS-R codes are presented in Fig. 5 together with experimental data [2] and recommended EL cross section. We note that in this particular case the Born approximation (the LOSS-R code) strongly overestimates experimental data at low and intermediate energies.

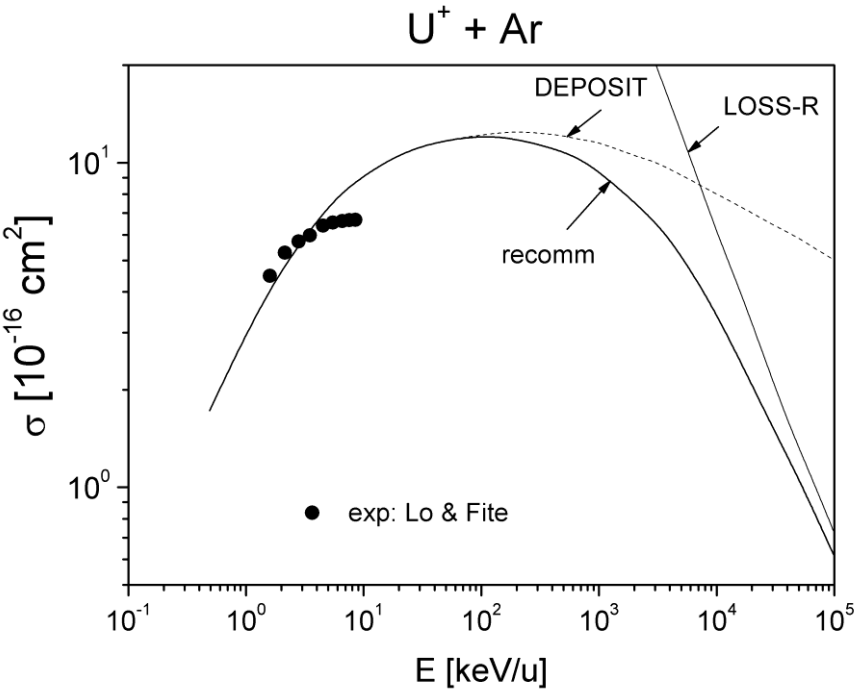

Fig. 5. Total electron-loss cross sections of U^+ ions by Ar atoms as a function of the ion energy. Experiment: solid circles – estimated from [2]. Theory: dashed curve – DEPOSIT code, thin solid curve – the LOSS-R code, thick solid curve – recommended cross section, eq. (28).

It is interesting to investigate the behavior of the total EL cross sections for collisions of highly charged ions with neutrals. The total EL cross sections for U^{28+} + Ar collisions are presented in Fig. 6 where available experimental data together with CTMC, the present semi-classical and Born calculations are given. It is seen that the recommended cross section is in good agreement with four experimental points.

In highly charged ions, the outermost electrons are already tightly bound (in this case of U^{28+} the ionization energy of the outermost electron is ~ 1 keV), and thus their radii tend to shrink toward a point-like charge (for U^{28+} the radius is 0.75 a_0 and for neutral He it is 0.93 a_0. i.e. of the same size, Table 1) instead of a large electron cloud and simultaneously their velocities can be too large to have multiple collision interactions in an single encounter. As the interaction time of projectile electrons with the target electron cloud becomes shorter, the effective numbers of collisions between projectile and target electrons decreases, and, therefore, the effective cross sections are drastically reduced.

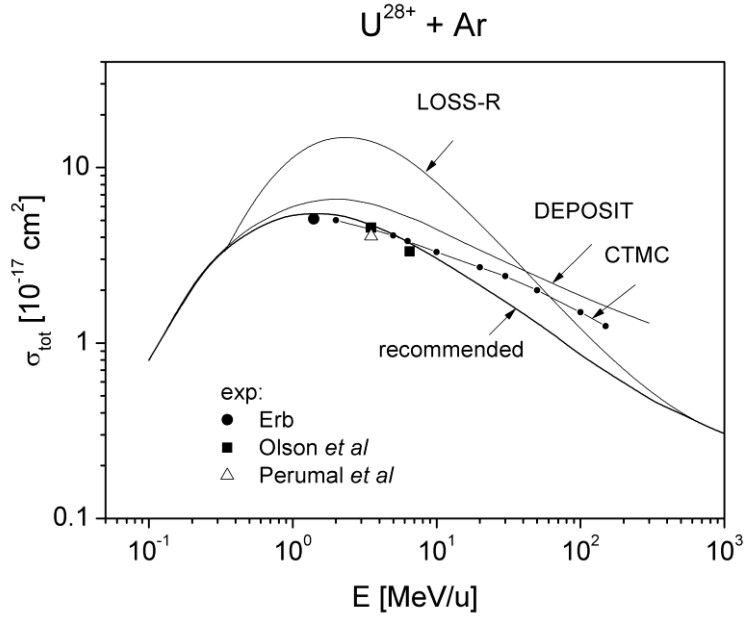

Fig. 6. Total EL cross sections of U^{28+} ions by Ar atoms as a function of the ion energy. Experiment: solid circle – [27], solid squares – [9]. Theory: solid curve with circles – CTMC [9], dashed curve – DEPOSIT code, thin solid curve – LOSS-R code, thick solid curve – recommended cross section, eq. (28).

The present version of the DEPOSIT code can be also applied for electron loss of negative ions by neutral atoms as seen in Fig. 7 where EL cross sections of Ge^- and Au^- by Ar atoms are given in comparison with experimental data [28, 29]. We can not present the Born results (and recommended data) at higher velocities, v > 3 a.u., since the Born cross sections are not available for these ions. The dashed curve for Au^- ions (right figure) is taken from the model [29] and represents a simple estimation of the EL cross section as a convolution of a free-electron scattering cross section and the velocity distribution of the outermost electron in the anion's rest frame.

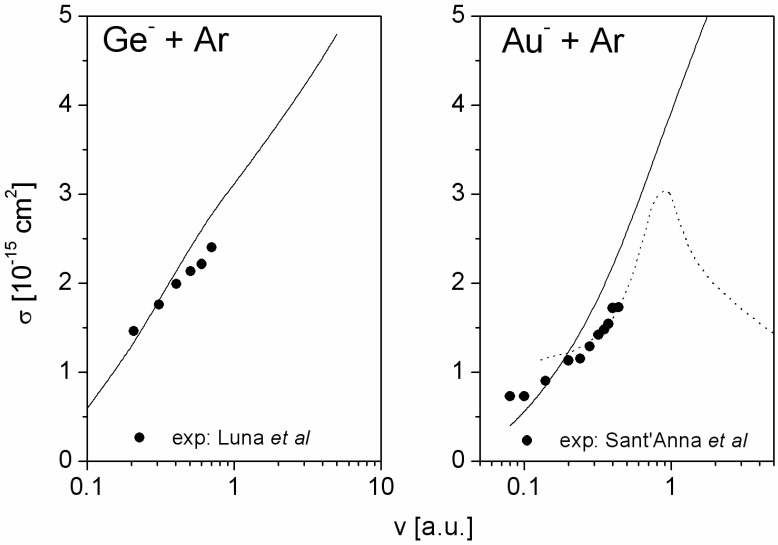

Fig. 7. Total electron-loss cross sections of Ge^- and Au^- ions by Ar atoms as a function of the ion energy. Experiment, solid circles: Ge^- [28], Au^- [32]. Theory: dotted curve – the model cross section from [29], solid curves – DEPOSIT code.

Figures 8 and 9 reproduce the EL and ionization cross sections of W and W^+ in collisions with neutral atoms, electrons and protons. These cross sections are of interest for plasma physics especially for ITER problems.

The total EL cross sections for W^+ ions colliding with H, He, Ar, W atoms and ionization cross sections in collisions with protons (p) and electrons (e) are shown in Fig. 8. The EL cross sections were calculated with the help of DEPOSIT and LOSS-R codes, one-electron ionization cross sections by protons using the LOSS-R code, one-electron ionization cross sections (1e) by electron impact using the ATOM code [23]; solid circles are the experimental 1e-cross sections from the work [30]. For comparison, the two-electron ionization cross sections (2e) induced by electron impact are also presented in the figure; the open circles are experimental data [31] and the solid curve corresponds to the semi-empirical formula given in [32].

Similar picture but for collisions of neutral W atoms with plasma particles is shown in Fig. 9.

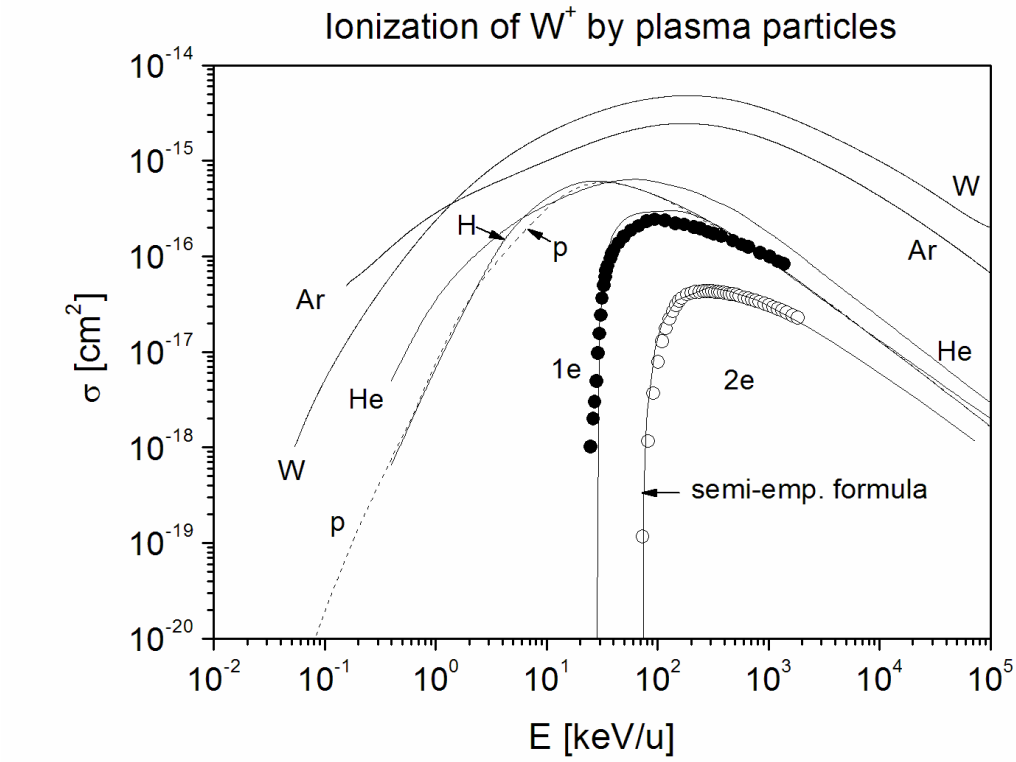

Fig. 8. Ionization cross sections of W^+ ions. Experiment: solid circles - single ionization cross sections by electron impact, from [30], open circles – double-electron ionization cross sections [31]. Theory: *e* and *p* - single ionization cross sections by electrons and protons, the ATOM and LOSS-R codes, respectively; H, He, Ar and W – total electron-loss cross sections by neutral atoms, recommended data, eq. (28); 2*e* – double-electron ionization cross sections by electron impact, semi-empirical formula given in [32]. Electron-impact ionization cross sections are given as a function of equivalent electron energy.

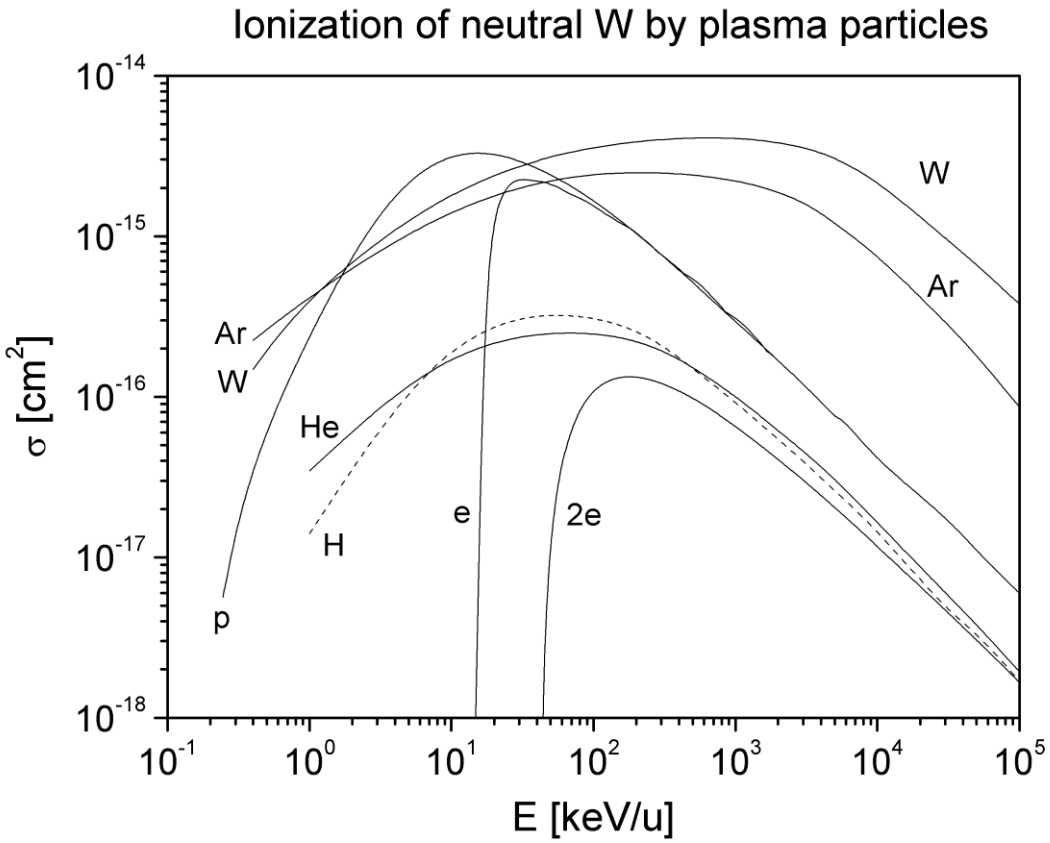

Fig. 9. Calculated EL and ionization cross sections of neutral W atoms: *e* and *p* - single ionization cross sections by electrons and protons, the ATOM and LOSS=R codes, respectively; H, He, Ar and W – total electron-loss cross sections by neutral atoms, recommended data, eq. (28); 2*e* – double-ionization cross section by electron impact, semi-empirical formula [32]. Electron-impact ionization cross sections are given as a function of equivalent electron energy.

4.2 Rate coefficients for ionization of W^+ and W projectiles

For plasma modeling and beam attenuation applications in plasmas, the main interest constitutes the electron-loss rate coefficients, i.e., $v\sigma$ values averaged over a Maxwellian velocity distribution function of the plasma particles.

Figures 10 and 11 show those for W^+ and W in collisions with plasma particles which are obtained from the cross-section data given in Figs. 8 and 9, respectively. From these figures, it is clear that the rate coefficients for EL of both W atoms and W^+ ions are far dominated by electron impact at and below the temperature of 100 eV which is close to that in divertor plasmas and in principle no other particles play any role at all in their electron losses. As the temperature increases up to 10 keV range which is relevant to the central part of the main plasmas, those by heavy particles sharply increase and dominate the electron contribution, as expected.

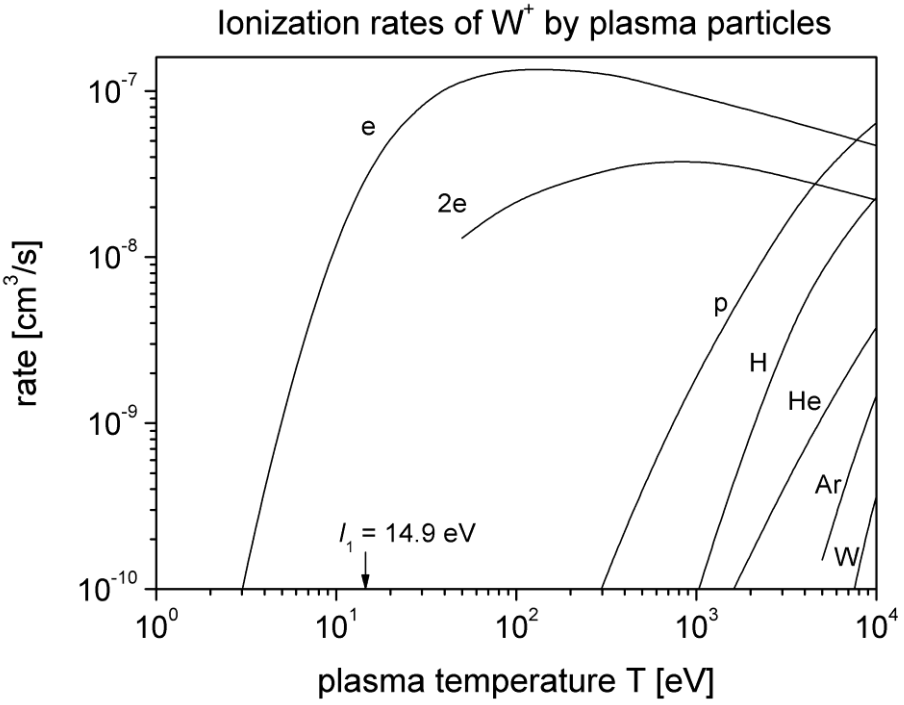

Fig. 10. Electron-loss rate coefficients of W^+ ions as a function of the particle temperature by neutral atoms (H, He, Ar and W), protons and electrons. e and 2e denote one- and two-electron impact ionization rate coefficients, and arrow indicates the ionization potential I_1 = 14.9 eV of W^+ ion.

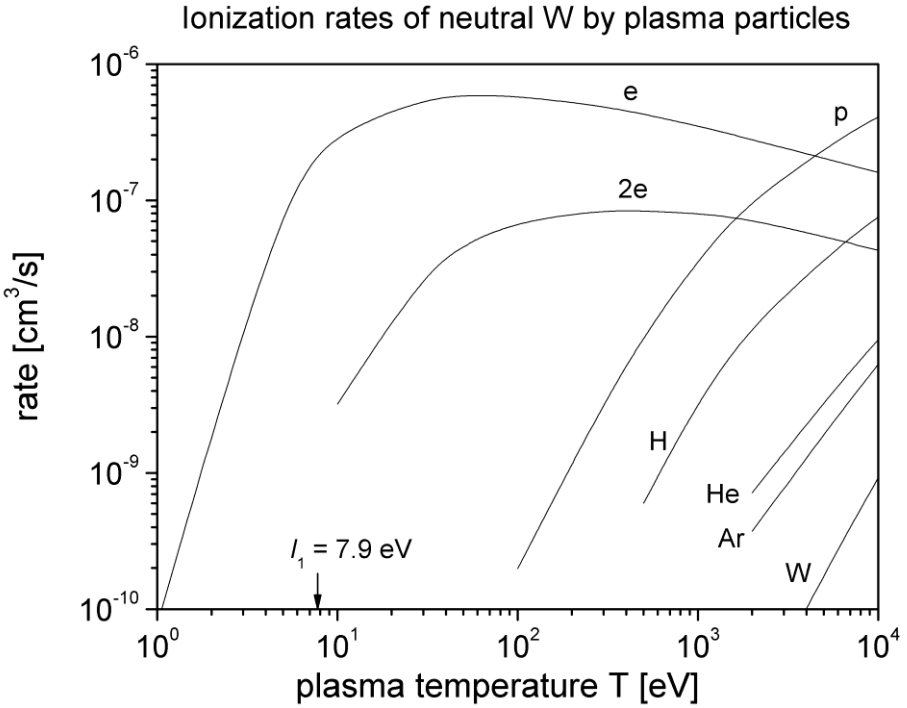

Fig. 11. Electron-loss rate coefficients of W atoms as a function of the particle temperature by neutral atoms (H, He, Ar and W), protons and electrons. e and 2e mean one- and two-electron impact ionization rate coefficients, and arrow indicates the ionization potential I_1 = 7.9 eV of W atom.

4.3 Multiple-electron loss cross sections at low energies.

The properties of the total and multiple-electron loss cross sections and probabilities of heavy ions colliding with neutrals are considered in several papers (see, e.g., [16], [19] and [33]). The data on multiple-electron loss cross sections at low energies are quite scarce. Typical multiple electron loss data for Ar^+ and U^+ ions in collisions with neutral Ar are compared with the present calculations in Figs. 12 and 13. The agreement between calculated and experimental data are reasonable within a factor of less than 2 keeping in mind hat these cases are so complicated to be handled theoretically.

It is found that, in both cases, sum of multiple-electron loss cross sections are comparable to or even larger than those of single electron loss. Therefore, they can not be neglected but play a key role in loss processes of heavy particles, particularly under heavy target atom collisions. This can also be the case for W atoms and ions which is our present interest, though there are no data available.

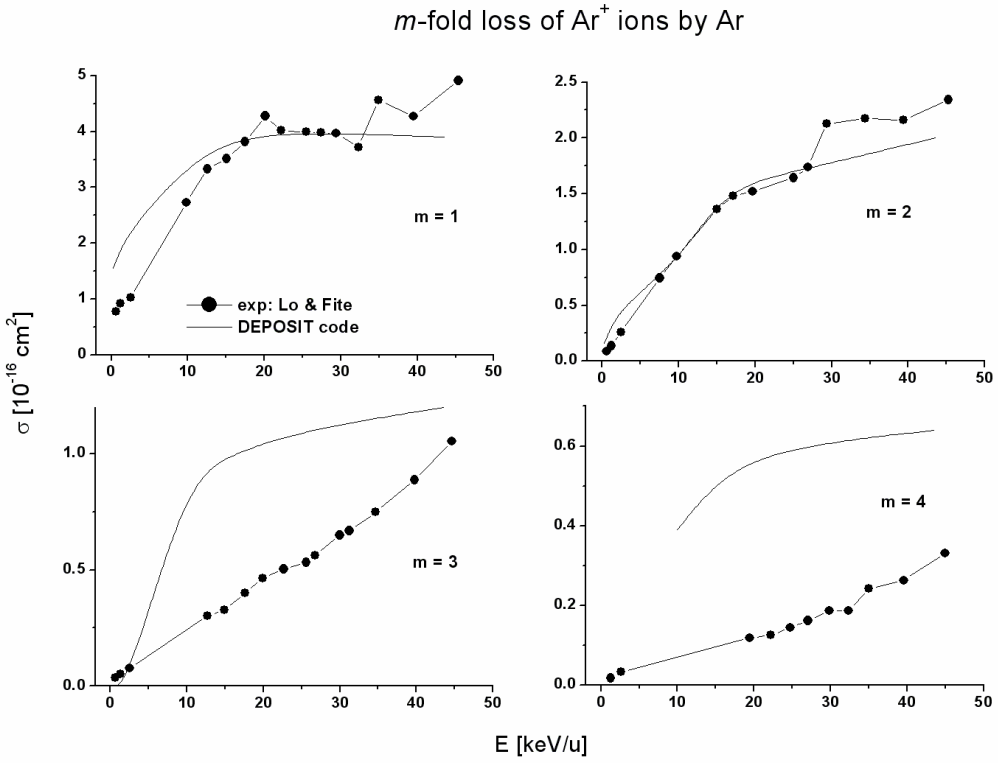

Fig. 12. The m-fold electron-loss cross sections of Ar^+ ions by Ar atoms. Experiment: solid circles – [2]. Theory: solid curves – the DEPOSIT code, present work.

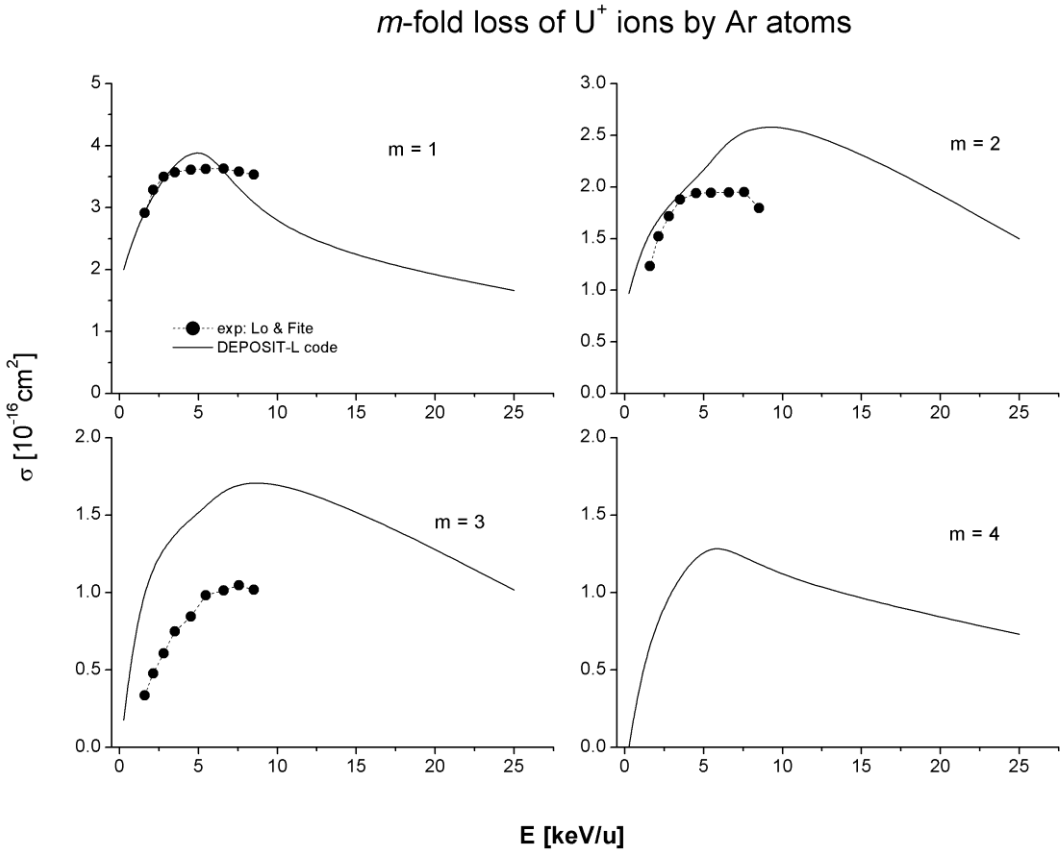

Fig. 13. The m-fold electron-loss cross sections of U^+ ions by Ar atoms. Experiment: solid circles – [2]. Theory: solid curves – the DEPOSIT code, present work.

Conclusion

The classical energy-deposition model, previously used to describe the total and multiple-electron loss cross sections of heavy ions at high-energy collisions with neutral atoms, is extended to apply it at low and intermediate energies using a new version of the DEPOSIT computer code.

It is found that the EL cross sections calculated by the DEPOSIT code for heavy (positive, negative ions and neutral) projectiles colliding with neutral atomic targets are in reasonable agreement (within a factor of 2) with available experimental and theoretical data at energies $E >$ 10 keV/u. Furthermore, calculated partial multiple-electron loss cross sections at very low energies are also found to be consistent with the observed data though the data themselves are very limited.

Combining the present results obtained by the DEPOSIT code at low and intermediate energies with the Born approximation results at high energies (the LOSS-R code), the cross sections for various ion-atom collisions are recommended over a wide range of the collision energies.

Acknowledgements
The work was partly performed under the RFBR grant Nr. 08-02-00005-a. This work is partially supported by the NIFS/NINS project of Foundation Network for Scientific collaboration.

REFERENCES

[1] Janev R K, Presnyakov L P and Shevelko V P 1985 *Physics of Highly Charged Ions* (Springer Berlin)
[2] Lo H H and Fite W L 1970 *At. Data* **1** 305
[3] Betz H D 1972 *Rev. Mod. Phys*. **44** 465
[4] Firsov O B 1958 Sov. Phys. – JETP **34** 306; *ibid* **36** 1076
[5] Russek A and Thomas M T 1958 *Phys. Rev*. **109** 2015
[6] Kishinevskii L M and Parilis E G 1962 *Sov. Phys. – Izvestiya AN SSSR* **26** 1410
[7] Komarov F F and Kumakhov M A 1973 *Phys. Stat. Sol.* **58** 389
[8] Olson R E, Watson R L, Horvat V, Zaharakis K E 2002 *J. Phys.* B **35** 1893
[9] Olson R E, Watson R L, Horvat V *et al* 2004 *J. Phys.* B **37** 4539
[10] DuBois R, Santos A C F, Olson R E et al 2003 *Phys. Rev*. A **68** 042701
[11] Bohr N 1915 Phil. Mag. **30** 581
[12] Russek A and Meli J 1970 *Physica* **46** 222
[13] Cocke C L 1979 *Phys. Rev*. A **20** 749
[14] Cocke C L and Olson R E 1991 *Phys. Rep*. **205** 153
[15] Solov'ev E A 1981 *Sov. Phys. - JETP* 1981 **54** 893
[16] Santos A C F and DuBois R D 2004 *Phys. Rev*. A **69** 042709
[17] Yamamura Y and Tawara H, 1996 *At. Data Nucl. Data Tables* **62** 149
[18] *Progress in the ITER Physics basics,* 2007 *Nuclear Fusion* 47 (IOP Publishing and IAEA)
[19] Shevelko V P, Litsarev M S and Tawara H 2008 *J. Phys.* B **41** 115204
[20] Beigman I L, Tolstikhina I Yu and Shevelko V P 2008 *Tech. Phys*. **53** 546
[21] Landau L and Lifshits E 1976 *Mechanics 3d. ed., Pergamon*
[22] Salvat F, Martinez J D, Mayol R and Parellada J 1987 *Phys. Rev*. A **36** 467
[23] Vainshtein L A and Shevelko V P 1993 *Atomic Physics for Hot Plasmas* (IOP, Bristol)
[24] Desclaux J P 1973 *Atom. Data Nucl. Data Tables* **12** 311
[25] Montanaru C C, Miraglia J E and Arista N R 2002 *Phys. Rev*. A **66** 042902; *ibid* 2009 A **79** 032903
[26] *http://www.gsi.de/fair/index_e.html*
[27] Erb W 1978 *GSI Report GSI-P-78, Darmstadt*
[28] Luna H, Zappa F, Martins M H et al 2003 *Phys. Rev.* A 68 042701
[29] Sant'Anna M M, Zappa F, Jalbert G et al 2009 *Plasma Phys. Control. Fusion* **51** 045707.
[30] Tawara H and Kato M 1999 *NIFS-DATA-51* (NIFS, Japan).
[31] Stenke M, Aichele K, Hathiramani D et al 1995 *J. Phys. B* **28** 4853
[32] Bélenger C, Defrance P, Salzborn E et al 1997 *J. Phys.* B **30** 2667.
[33] Song M-Y, Litsarev M S, Shevelko V P and Tawara H 2009 *Nucl. Instrum. Meth*. B **267** 2369